Available online at www.sciencedirect.com
SCIENCE DIRECT®
Composites Science and Technology 66 (2006) 2491–2499
COMPOSITES SCIENCE AND TECHNOLOGY
www.elsevier.com/locate/compscitech

Lay-up independent fracture criterion for notched laminated composites

Bokwon Lee [1], Bhavani V. Sankar *,[2]

Department of Mechanical and Aerospace Engineering, University of Florida, P.O. Box 116250, Gainesville, FL 32611, USA

Received 10 January 2006; accepted 11 January 2006
Available online 6 March 2006

Abstract

The purpose of this study was to investigate the applicability of an existing lay-up independent fracture criterion for notched composite laminates. A detailed finite element analysis of notched graphite/epoxy laminates was performed to understand the nature of stresses and crack tip parameters in finite-width composite panels. A new laminate parameter β, which plays a crucial role in the fracture of laminated composites, has been identified. The effects of blunt crack tip and local damage on fracture behavior of notched composite laminates are investigated using the finite element analysis. The results of experiments performed elsewhere are analyzed in the light of new understanding of crack tip stress field, and the applicability of the lay-up independent fracture criterion for notched composite laminates is discussed. It is found that a lay-up independent fracture model that considers local damage effects provides good correlation with the experimental data.

Keywords: Composite laminates; Finite elements; B. Fracture; B. Fracture toughness; Graphite/epoxy; Laminated composites; Notched composites; Stress intensity factor

1. Introduction

Several failure models have been developed for the prediction of notched strength of composite laminates. An extensive review of these models can be found in Awerbuch and Madhukar [1]. Failure behavior of notched composite laminates depends on a variety of factors, the most important being laminate configuration, specimen geometry and notch shape. Due to the complex fracture behavior in the vicinity of the notch, a number of assumptions and approximations are made in the most commonly used failure models. Most of the popular models are based on the characteristic length concept originally proposed by Whitney and Nuismer [2]. One limitation of these models is that the characteristic length is not a material system property, but depends on factors such as laminate configuration, thickness, etc. In other words, the characteristic length estimated from tests on one laminate configuration cannot be used to predict the fracture of other laminates of the same material system. Recently, Sun et al. [3,4] employed linear elastic fracture mechanics (LEFM) concepts to develop a lay-up independent fracture criterion. This criterion requires the existence of one or more plies with fibers parallel to the loading direction, and this ply is called the load-carrying ply. The main principle of their model is that the failure of fibers in the load-carrying ply governs the failure of the entire laminate. The stress intensity factor in the load-carrying ply that causes fiber breakage was considered as the principal fracture parameter. One of the main advantages of the lay-up independent model is that a single fracture parameter, fracture toughness of the load-carrying ply (K_Q^L), is used to predict the failure of laminates with different laminate configurations. However, as mentioned earlier, this theory requires the presence of plies with fiber orientation parallel to the loading direction.

The purpose of this study was to further verify and also improve the existing lay-up independent fracture criterion for notched composite laminates. In that process an

* Corresponding author. Tel.: +1 352 392 6749; fax: +1 352 392 7303.
E-mail address: sankar@ufl.edu (B.V. Sankar).
[1] Graduate student.
[2] Newton C. Ebaugh professor.

0266-3538/$ - see front matter © 2006 Published by Elsevier Ltd.
doi:10.1016/j.compscitech.2006.01.014

empirical relation for finite width correction factor for orthotropic laminates has also been developed. Detailed finite element analyses, both two- and three-dimensional models, of the laminates used in the experimental study of Sun and Vaidya [3] were performed to estimate the average laminate stresses as well as stresses in individual layers near the crack tip. An analytical model for determining the stress intensity factor in the load-carrying ply is also developed, and the difference between the present approach and that of Sun et al. [3,4] is discussed. It has been found that factors such as crack bluntness, delamination and fiber splitting in the crack tip region play a significant role in reducing the stresses in the angle plies, and thus increasing the stresses and hence the stress intensity factor in the load-carrying ply. A new laminate parameter, referred to as β, has been identified. This parameter represents the ratio of the axial stresses to the normal stresses at points straight ahead of the crack tip, and plays a crucial role in the failure of notched laminates. This parameter, which is only a function of the laminate stiffness coefficients, also appears in the expression for finite width correction factor for orthotropic laminates.

2. Experimental background

As mentioned earlier we have analyzed the results of fracture tests performed by Sun et al. [3,4]. The material properties, laminate configurations used and respective failure loads are presented here for the sake of completion. Nine different laminate configurations made from AS4/3501-6 (Hercules) graphite/epoxy were tested. The material properties of this unidirectional prepreg tape are: $E_L = 138$ GPa; $E_T = 9.65$ GPa; $G_{LT} = 5.24$ GPa; $\nu_{LT} = 0.3$; and ply thickness = 0.127 mm. The panel specifications, geometry, and coordinate system used for the present analysis are shown in Fig. 1. The specimens were fabricated using the hand lay-up technique and cured in an autoclave. Each of the symmetric laminate configuration studied had at least two principal load carrying plies (0° plies), i.e., plies with fibers aligned along the loading direction.

The fracture toughness estimated using the nominal or average stress intensity factor for the laminate is shown under the column "Laminate fracture toughness" $\overline{K}_Q$ in Table 1. This is computed using the formula

$$\overline{K}_Q = \sigma_y^{\infty} Y(a/w)\sqrt{\pi a} \tag{1}$$

where σ_y^{∞} is the remote stress at the instant of failure, $2a$ is the crack length, $2w$ is the specimen width and Y is the finite width correction factor. Sun et al. [3,4] used the Y for isotropic materials, which is equal to 1.0414 for the present case ($a/w = 0.2627$). One can note from Table 1 that the values of fracture toughness estimated using this method is not the same for the different laminates, and hence cannot be considered as a material property. The average value of the laminate fracture toughness $\overline{K}_Q$ was 50.44 MPa$\sqrt{\text{m}}$ and the standard deviation was 17.68 MPa$\sqrt{\text{m}}$.

3. Stress intensity factor calculations

3.1. Average or laminate stress intensity factor

The average stress intensity factor for a laminate is calculated assuming that the laminate is a homogeneous material of some hypothetical orthotropic or anisotropic material. The average stress intensity factor $\overline{K}_I$ for notched laminates can be calculated using three different methods as follows:

1. Using the remote stress in Eq. (1).
2. Finite element analysis I: From the normal stress distribution ahead of the crack tip obtained from a finite element model using the equation

$$\overline{K}_I = \lim_{r\to 0} \bar{\sigma}_{yy}(r,0)\sqrt{2\pi r} \tag{2}$$

where r is the distance from the crack tip and normal stress component $\bar{\sigma}_{yy}$ is the average stress in the laminate. In Eq. (2) the over bar in $\overline{K}_I$ denotes that it is the average stress intensity factor for the laminate.
3. Finite element analysis II: From the J-integral calculated from the finite element models. The relation between energy release rate and stress intensity factor for orthotropic materials is given by [5]:

$$J = \overline{G}_I = \overline{K}_I^2 \left(\frac{a_{11}a_{22}}{2}\right)^{1/2} \left[\left(\frac{a_{22}}{a_{11}}\right)^{1/2} + \frac{2a_{12}+a_{66}}{2a_{11}}\right]^{1/2} \tag{3a}$$

where a_{ij} are the coefficients in the compliance matrix of the plane orthotropic material and they can be expressed

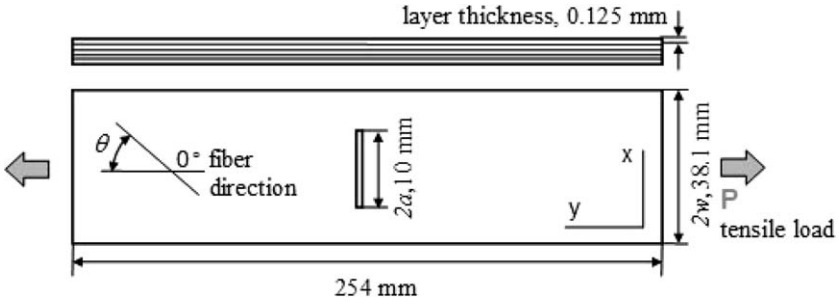

Fig. 1. Specimen dimensions and definition of fiber orientation.

Table 1
Fracture toughness of various graphite epoxy laminates

Specimen ID	Laminate configuration	Failure stress (MPa)	Laminate fracture toughness $\overline{K}_Q$ (MPa$\sqrt{\text{m}}$)
S1	$[0/90/\pm45]_s$	343.00	44.83
S2	$[\pm45/90/0]_s$	323.27	42.19
S3	$[90/0/\pm45]_s$	316.05	41.25
S4	$[0/\pm15]_s$	695.84	90.82
S5	$[0/\pm30]_s$	466.14	60.84
S6	$[0/\pm45]_s$	351.14	45.83
S7	$[0/90]_{2s}$	446.76	58.31
S8	$[\pm45/0/\pm45]_s$	287.16	37.48
S9	$[\pm45_2/0/\pm45]_s$	248.40	32.42
Average laminate fracture toughness			50.44
Standard deviation			17.68

in terms of the elastic constants. The definition of a_{ij} can be understood from the strain–stress relations shown below:

$$\begin{aligned}\varepsilon_{xx} &= a_{11}\sigma_{xx} + a_{12}\sigma_{yy} + a_{16}\tau_{xy}\\ \varepsilon_{yy} &= a_{12}\sigma_{xx} + a_{22}\sigma_{yy} + a_{26}\tau_{xy}\\ \gamma_{xy} &= a_{16}\sigma_{xx} + a_{26}\sigma_{yy} + a_{66}\tau_{xy}\\ \sigma_{xz} &= \sigma_{yz} = \sigma_z = 0\end{aligned} \tag{3b}$$

It should be mentioned that the aforementioned elastic constants and hence the compliance coefficients are calculated from the extensional stiffness matrix $[A]$ of the laminate. When the remote applied stress corresponds to the failure stress observed in tests, the stress intensity factor $\overline{K}_I$ becomes the fracture toughness $\overline{K}_Q$.

3.2. Derivation of stress intensity factor in the load-carrying ply

The stress intensity factor of the load-carrying ply, K_I^L, can be estimated using two different methods.

1. From the average stress intensity factor $\overline{K}_I$ and using and the classical lamination theory for calculating the portion of the stresses carried by the load-carrying ply. This procedure is described in the succeeding section.
2. Same procedure as in Eq. (2) but using normal stress field in the load-carrying ply extracted from the finite element model:

$$K_I^L = \lim_{r\to 0}\sigma_{yy}^L(r,0)\sqrt{2\pi r} \tag{4}$$

In Eq. (4) the superscript L denotes the load-carrying ply.

In this section, we derive an analytical expression for the stress intensity factor in the load-carrying ply in terms of the average laminate stress intensity factor obtained using three methods mentioned earlier. The derivation of stress intensity factor presented here is based on LEFM and classical lamination theory. The state of stress in the vicinity of a crack in an orthotropic material is given by [5]:

$$\bar{\sigma}_{yy}(r,0) = \frac{\overline{K}_I}{\sqrt{2\pi r}}\text{Re}[1] \tag{5a}$$

$$\bar{\sigma}_{xx}(r,0) = \frac{\overline{K}_I}{\sqrt{2\pi r}}\text{Re}[-s_1 s_2] \tag{5b}$$

where the parameters s_1 and s_2 are related to the equivalent orthotropic elastic constants of the laminate as [5]

$$\begin{aligned}s_1 s_2 &= -\left(\frac{a_{22}}{a_{11}}\right)^{1/2}\\ s_1 + s_2 &= \mathrm{i}\sqrt{2}\left[\left(\frac{a_{22}}{a_{11}}\right)^{1/2} + \left(\frac{2a_{12}+a_{66}}{2a_{11}}\right)\right]^{1/2}\end{aligned} \tag{5c}$$

We will use a new laminate parameter β to denote the ratio between the two normal stresses shown in Eqs. (5a) and (5b),

$$\beta = \frac{\bar{\sigma}_{xx}(r,0)}{\bar{\sigma}_{yy}(r,0)} = \text{Re}[-s_1 s_2] \tag{6}$$

It should be noted that β is a property of the laminate or equivalent orthotropic elastic constants, and does not depend on the loading. The values of β for the various laminates used in this study are listed in Table 2. The value of β for isotropic materials is unity. We will use the classical lamination theory to extract the stresses in the load-carrying ply from the force resultants in the vicinity of the crack tip. In the case of symmetric laminated plates without coupling, the force/mid-plane strain equations can be expressed in matrix form as

$$\begin{Bmatrix} N_x\\ N_y\\ N_{xy}\end{Bmatrix} = \begin{bmatrix} A_{11} & A_{12} & A_{16}\\ A_{12} & A_{22} & A_{26}\\ A_{16} & A_{26} & A_{66}\end{bmatrix}\begin{Bmatrix}\varepsilon_x^0\\ \varepsilon_y^0\\ \gamma_{xy}^0\end{Bmatrix} \tag{7}$$

where $[A]$ is the laminate extensional stiffness matrix. The inverse relation is given by

$$\begin{Bmatrix}\varepsilon_x^0\\ \varepsilon_y^0\\ \gamma_{xy}^0\end{Bmatrix} = \begin{bmatrix} A_{11}^* & A_{12}^* & A_{16}^*\\ A_{12}^* & A_{22}^* & A_{26}^*\\ A_{16}^* & A_{26}^* & A_{66}^*\end{bmatrix}\begin{Bmatrix} N_x\\ N_y\\ N_{xy}\end{Bmatrix} \tag{8}$$

where superscript $*$ denotes the component of $[A^{-1}]$. The stresses in the load-carrying ply can be derived from the mid-plane strains as

$$\begin{Bmatrix}\sigma_{xx}^L\\ \sigma_{yy}^L\\ \tau_{xy}^L\end{Bmatrix} = \begin{bmatrix}\overline{Q}_{11}^L & \overline{Q}_{12}^L & \overline{Q}_{16}^L\\ \overline{Q}_{12}^L & \overline{Q}_{22}^L & \overline{Q}_{26}^L\\ \overline{Q}_{16}^L & \overline{Q}_{26}^L & \overline{Q}_{66}^L\end{bmatrix}\begin{Bmatrix}\varepsilon_x^0\\ \varepsilon_y^0\\ \gamma_{xy}^0\end{Bmatrix} \tag{9}$$

Table 2
Fracture toughness of the load-carrying ply for various laminates evaluated using two different analytical methods

Notation	Laminate configuration	Laminate parameter β	Fracture toughness of the load-carrying ply $K^L_{Q(A)}$ (MPa$\sqrt{\text{m}}$)	Fracture toughness of the load-carrying ply $K^L_{Q(B)}$ (MPa$\sqrt{\text{m}}$)
S1	$[0/90/\pm45]_s$	1	81.99	115.66
S2	$[\pm45/90/0]_s$	1	73.53	108.82
S3	$[90/0/\pm45]_s$	1	75.08	106.43
S4	$[0/\pm15]_s$	0.285	95.95	101.81
S5	$[0/\pm30]_s$	0.396	65.87	101.00
S6	$[0/\pm45]_s$	0.656	61.17	106.32
S7	$[0/90]_{2s}$	1	106.13	109.04
S8	$[\pm45/0/\pm45]_s$	0.767	56.25	119.81
S9	$[\pm45_2/0/\pm45]_s$	0.823	51.21	123.64
Average			74.13	110.28
Standard deviation			18.18	7.83

where the quantities $\overline{Q}^L_{ij}(i,j=1,2,6)$ are the stiffness coefficients of the principal load carrying plies. Substituting Eq. (8) into Eq. (9) yields the following equation:

$$\begin{Bmatrix}\sigma^L_{xx}\\ \sigma^L_{yy}\\ \tau^L_{xy}\end{Bmatrix}=\begin{bmatrix}\overline{Q}^L_{11} & \overline{Q}^L_{12} & \overline{Q}^L_{16}\\ \overline{Q}^L_{12} & \overline{Q}^L_{22} & \overline{Q}^L_{26}\\ \overline{Q}^L_{16} & \overline{Q}^L_{26} & \overline{Q}^L_{66}\end{bmatrix}\begin{bmatrix}A^*_{11} & A^*_{12} & A^*_{16}\\ A^*_{12} & A^*_{22} & A^*_{26}\\ A^*_{16} & A^*_{26} & A^*_{66}\end{bmatrix}\begin{Bmatrix}N_x\\ N_y\\ N_{xy}\end{Bmatrix} \tag{10}$$

In the vicinity of the crack tip the force resultants can be written in terms of the average stresses in the orthotropic laminate as

$$N_x=t\bar{\sigma}_{xx}=t\beta\bar{\sigma}_{yy},\quad N_y=t\bar{\sigma}_{yy},\quad N_{xy}=t\bar{\tau}_{xy}=0 \tag{11}$$

where t is the total thickness of laminate, and the parameter β has been defined in Eq. (6). Substituting from Eq. (11) into Eq. (10) we obtain the stresses in the load-carrying ply as

$$\begin{Bmatrix}\sigma^L_{xx}\\ \sigma^L_{yy}\\ \tau^L_{xy}\end{Bmatrix}=\begin{bmatrix}\overline{Q}^L_{11} & \overline{Q}^L_{12} & \overline{Q}^L_{16}\\ \overline{Q}^L_{12} & \overline{Q}^L_{22} & \overline{Q}^L_{26}\\ \overline{Q}^L_{16} & \overline{Q}^L_{26} & \overline{Q}^L_{66}\end{bmatrix}\begin{Bmatrix}A^*_{11}\beta+A^*_{12}\\ A^*_{12}\beta+A^*_{22}\\ A^*_{16}\beta+A^*_{26}\end{Bmatrix}(t\bar{\sigma}_{yy}) \tag{12}$$

In particular we are interested in the stress component σ^L_{yy} responsible for fracture and it is obtained from Eq. (12) as

$$\sigma^L_{yy}=[\overline{Q}^L_{12}(A^*_{11}\beta+A^*_{12})+\overline{Q}^L_{22}(A^*_{12}\beta+A^*_{22})](t\bar{\sigma}_{yy}) \tag{13}$$

Then the stress intensity factor K^L_I in the load-carrying ply can be expressed in terms of the laminate stress intensity factor $\overline{K}_I$ using a relation similar to that in Eq. (13)

$$K^L_{I(A)}=t[\overline{Q}^L_{12}(A^*_{11}\beta+A^*_{12})+\overline{Q}^L_{22}(A^*_{12}\beta+A^*_{22})]\overline{K}_I \tag{14}$$

In deriving Eq. (14) we have used the relation $K^L_I/\overline{K}_I=\sigma^L_{yy}/\bar{\sigma}_{yy}$. Note that the stress intensity factor calculated using Eq. (14) is denoted with a subscript $A(K^L_{I(A)})$ to distinguish it from the method followed by Sun et al. [3,4], which is described below. The fracture toughness evaluated using the proposed method will be denoted by $K^L_{Q(A)}$, and this can be related to the average laminate fracture toughness by an equation similar to Eq. (14) as follows:

$$K^L_{Q(A)}=t[\overline{Q}^L_{12}(A^*_{11}\beta+A^*_{12})+\overline{Q}^L_{22}(A^*_{12}\beta+A^*_{22})]\overline{K}_Q \tag{14a}$$

Sun and Vaidya [3] used a similar approach to calculate the stress intensity factor in the load-carrying ply, but they used the remote stresses applied to the laminate in order to determine the ratio of $\bar{\sigma}_{xx}/\bar{\sigma}_{yy}$ in the vicinity of the crack tip. Since the applied load is uniaxial, this ratio was equal to zero in their case. This is equivalent to taking the factor β as equal to zero. It should be emphasized that this stress ratio is not equal to zero in the vicinity of the crack tip, as there is a nonzero component of $\bar{\sigma}_{xx}$ is present (see Eq. (5b)). We denote this fracture toughness calculated by Sun and Vidya as $K^L_{Q(B)}$ (with a subscript B). Thus the relation between the ply fracture toughness $K^L_{Q(B)}$ and the laminate fracture toughness $\overline{K}_Q$ can be obtained by setting $\beta=0$ in Eq. (14a) and it takes the form:

$$K^L_{Q(B)}=t[\overline{Q}^L_{12}A^*_{12}+\overline{Q}^L_{22}A^*_{22}]\overline{K}_Q \tag{15}$$

4. Results and discussion

The values of the laminate parameter β and the load-carrying ply fracture toughness values $K^L_{Q(A)}$ and $K^L_{Q(B)}$ are shown in Table 2 for the nine laminate configurations. The average values and corresponding standard deviation are 74.35 MPa$\sqrt{\text{m}}$ and 18.35% for $K^L_{Q(A)}$, and 110.28 MPa$\sqrt{\text{m}}$ and 7.83% for $K^L_{Q(B)}$. Surprisingly, the case B wherein the β value was taken as zero, yielded consistent layer independent fracture toughness compared to the case A where the actual

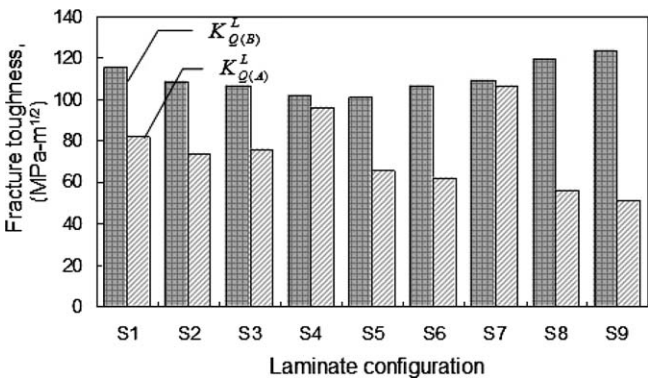

Fig. 2. Comparison of the fracture toughness of the load-carrying ply obtained using two different analytical methods.

stress ratio ($\beta > 0$) was used. Fig. 2 compares the two fracture toughness values for various laminate configurations.

The aforementioned analyses are approximate, since they do not consider any stress redistribution caused by physical fracture behavior such as local damage in the form of matrix cracking, delamination, etc. In order to fully understand the nature of crack tip stress field in finite-width laminates a detailed finite element analysis was performed. The procedures and the results are discussed in the following sections.

5. Finite element analysis

A detailed finite element analysis of the notched laminated composites was conducted in order to understand the stress field near the crack tip in finite width laminates. The purpose of the finite element analysis was to develop a model that could predict the fracture parameters of notched laminated composites, and to investigate the effect of local damage and crack tip shape on the stress intensity factor of notched laminated composites. Another goal of the study was to determine the orthotropic finite-width correction factor using the *J*-integral. The commercial FE package, ABAQUS® 6.2 [6], was used to analyze the various test specimens. Two types of analyses were performed. In the 2D (two-dimensional) model the specimens were modeled as orthotropic laminates. In the second model, 3D (three-dimensional) solid elements were used to model the individual layers of the laminate. In both cases sub-modeling was performed to improve the accuracy of the calculated crack tip parameters such as stress intensity factor and *J*-Integral. The mode *I* stress intensity factor, K_I, can be calculated using two different methods from the results of FE analysis as described in Section 3.2. However, the stress intensity factor of the load-carrying ply can be calculated only from the stresses $\sigma^L_{yy}(r,0)$ ahead of the crack tip using Eq. (4), because ABAQUS cannot calculate the *J*-integral at ply level. Further, the *J*-integral is not path independent for three-dimensional cracks and a zero-area contour has to be used to determine the point-wise energy release rate [7].

The stress intensity factors obtained using the above methods from two types of FE models are compared with the analytical models in the subsequent section. It is noted that overall analysis procedure and detailed results are presented for the case of $[0/\pm 45]_s$ laminate (Laminate S6), but a summary of the results for other eight laminate configurations are presented.

5.1. Two-dimensional finite element global model

The purpose of the 2D analysis is to compare the results with the analytical model so that the effect of finite-width of the specimen can be understood. Further FE models can be used to understand the effects of blunt crack tip and also other forms of damage such as delamination and fiber splitting. The various laminate configurations with center notch were modeled with eight node plane stress elements (CPS8R element). A quarter model was used, with symmetric boundary conditions. The width of the model, *w*, was 19.05 mm, and the length was 254 mm. The notch was modeled as a sharp crack with a half width $a = 5$ mm. Since the lay-up is symmetric, it was only necessary to model half of the thickness.

The main difference between global model and sub-model is mesh refinement. The FE global model uses relatively coarse mesh compared to the FE sub models. A fixed element size with width of 1 mm was used away from the crack tip in the FE global model. A relatively fine mesh was used adjacent to the notch. The geometry and the finite element models were created using ABAQUS/CAE modeling tool and ABAQUS keyword editor. Fig. 3 shows the initial mesh of the upper left quadrant. Separate elements were used to represent each ply and common nodes were used for interface of plies. The material property of each ply was modeled as a homogeneous linear elastic orthotropic material throughout this FE analysis. In order to use a single global coordinate system, the material properties of angle plies were transformed using the transformation relation for engineering constants. Orthotropic properties for AS4/3501-6 graphite/epoxy unidirectional lamina were defined as given in Section 2. The material property of each angle ply was implemented in ABAQUS by means of user material subroutine (UMAT). The fixed grip loading condition was simulated by constraining the nodes along the edge of the plate to have the same displacement under an applied load. This was also implemented by using the EQUATION command. The failure load obtained from experiments (see Table 1) was applied.

5.2. Two-dimensional finite element sub-model

The analysis was repeated with a very refined element size in order to investigate the local behavior and the sensitivity of the results to mesh refinement. All other aspects of the analysis were kept the same as the global model. For efficiency of computation, the finite element sub-modeling analysis technique was adopted. The sub-modeling analysis is most useful when it is necessary to obtain an accurate, detailed solution in a local area region based on interpolation of the solution from an initial, relatively coarse, global model. The sub-model is run as a separate analysis. The link between the sub-model and the global model is the transfer of results saved in the global model to the relevant boundary nodes of the sub-model. Thus, the response at the boundary of the sub-model is defined by the solution of the global model.

5.3. Comparison of results from the FE and analytical models

The stress intensity factor in the load-carrying ply was calculated using both the global and sub-model. The

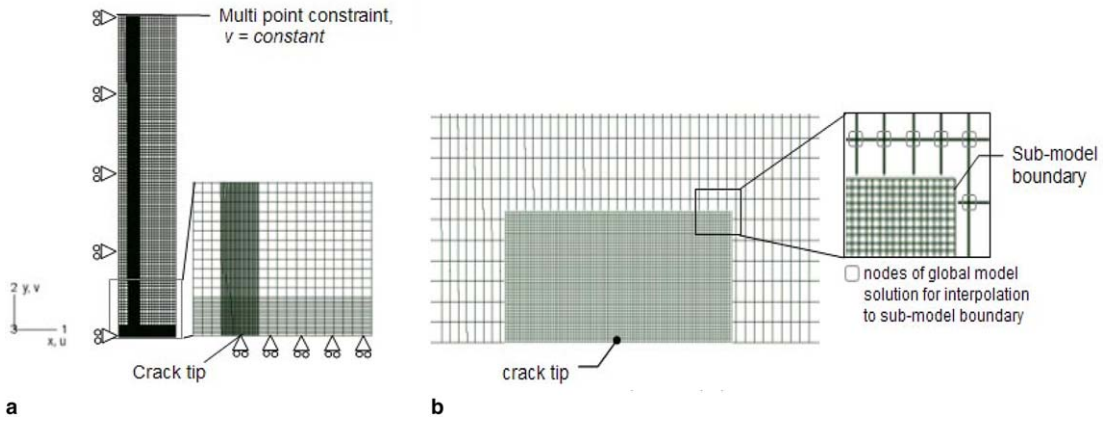

Fig. 3. Finite element mesh and boundary conditions: (a) global model; (b) sub-model.

laminate stress intensity factors calculated from the two models were in good agreement for all the laminate configurations indicating that the mesh refinement was sufficient. From the laminate stress intensity factor we can calculate the finite width correction factor Y using Eq. (1). The values of Y for various laminate configurations are shown as a function of a/w and β in Fig. 4. It has been found that the finite width correction factor is a strong function of the newly introduced lamination parameter β. An empirical relation for Y was derived as follows:

$$Y\left(\frac{a}{w}\right) = 1 + b_1\left(\frac{a}{w}\right)(1 + c_1B + c_2B^2) + b_2\left(\frac{a}{w}\right)^2 \times (1 + c_3B + c_4B^2) + b_3\left(\frac{a}{w}\right)^3(1 + c_5B + c_6B^2) \tag{16}$$

where $B = 1 - \beta$. The values of various constants in the above equation are listed in Table 3. More on the finite-width correction factor for orthotropic laminates and the significance of β will be published elsewhere. Finite-width correction factors for central openings other than cracks in a general anisotropic laminate have been derived by Tan [8].

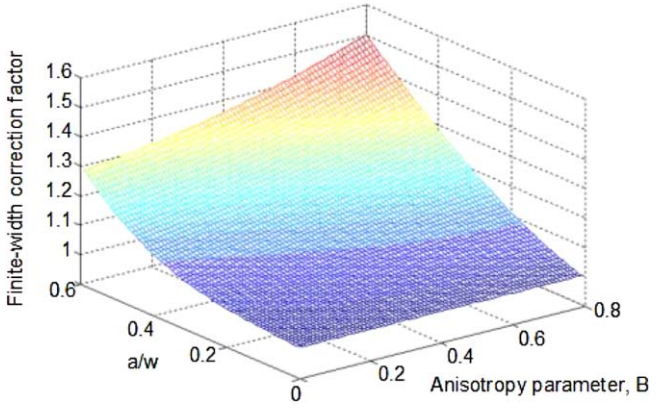

Fig. 4. The finite width correction factors as a function of anisotropy parameter B and ratio of crack size to panel width a/w. Note that the parameter B is related to β by $B = 1 - \beta$.

Figs. 5a and b, respectively, show $\sigma^L_{yy}\sqrt{2\pi r}$ and $\sigma^L_{xx}\sqrt{2\pi r}/\beta$ distribution in FE global and sub-models. Ideally the two curves should extrapolate to a same value at $r = 0$, which is equal to the layer fracture toughness K^L_Q. However, in the global model, the former line extrapolates to $K^L_{Q(B)}$ and the latter line predicts a much lower value of fracture toughness. The result indicates that the coarse mesh of global model does not have sufficient nodes to capture the effects of σ_{xx}. On the other hand, in the sub model (Fig. 5b) both lines extrapolate to $K^L_{Q(A)}$ for the laminate under consideration.

The results for the load-carrying ply fracture toughness K^L_Q for all laminate configurations are summarized in Fig. 6 and compared with the two analytical models. The $K^L_{Q(B)}$ calculated from Eq. (15) agree well with the results of global model, which has a relatively coarse mesh. On the other hand, the $K^L_{Q(A)}$ calculated from the exact LEFM solution, Eq. (14), show good agreement with the results of sub-model, which has a very fine mesh. It is obvious from the results that the σ_{xx} stresses ahead of the crack tip play a significant role in the estimation of K^L_Q.

5.4. Effect of blunt crack tip

The LEFM assumes the existence of a sharp crack, and the SIF is calculated on the basis of ensuing singular stress field. However, we would like to investigate the effect of blunt crack tip on the stress field and on the effective stress intensity factor. This is akin to considering a small scale yield zone at the crack tip and calculating the effective stress intensity factor using models such as Dugdale's. According to the specimen preparation process [3] the crack was made by water jet cut and further extended with a 0.2 mm thick jeweler's saw blade. Thus, in the present analysis, the crack tip thickness was assumed less than 0.2 mm and the crack tip shape was assumed elliptical, triangular, and rectangular, respectively. These assumptions were carefully investigated through the series of FE sub-models and the results are discussed below for the case of $[0/\pm45]_s$ laminates.

Table 3
The coefficients in the semi-empirical formula for orthotropic finite-width correction factor

b_1	c_1	c_2	b_2	c_3	c_4	b_3	c_5	c_6
0.1091	5.0461	−2.1324	−0.2319	−2.9103	−4.4927	1.4727	−1.5124	−0.0375

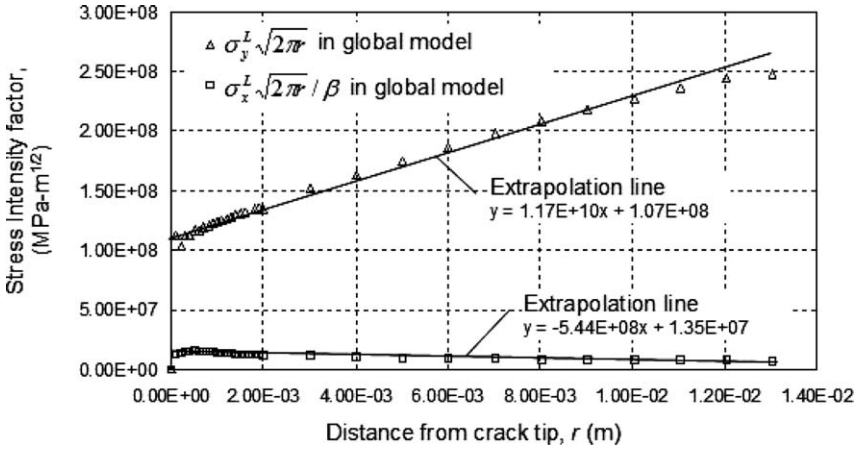

Fig. 5. $\sigma_{yy}\sqrt{2\pi r}$ and $\sigma_{xx}\sqrt{2\pi r}/\beta$ distribution in the global model for $[0/\pm 45]_s$ laminates.

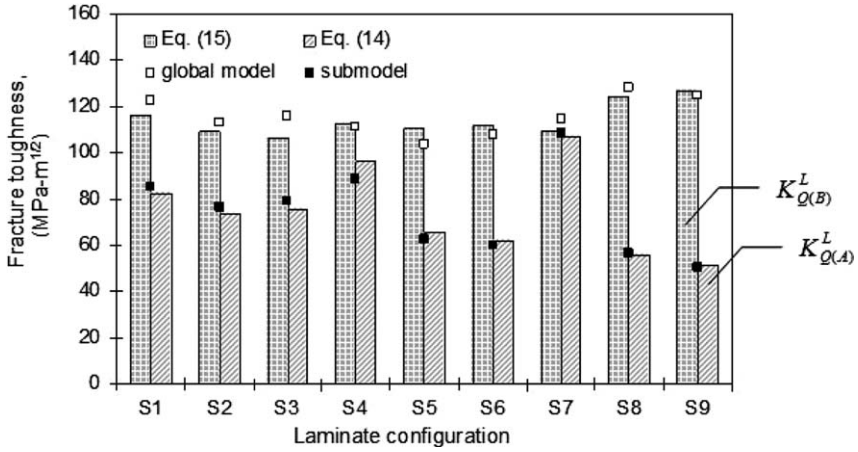

Fig. 6. Comparison of fracture toughness of the principal load-carrying ply obtained using the global model and the sub-model.

Fig. 7 compares the effect of notch tip profile and notch width on the stress intensity factor of the load carrying ply using global and sub-models. From the results of the global model, it is evident that stress intensity factors of global model are not greatly influenced by crack tip shape.

However, the results of the sub-model indicate that the crack tip shape has a significant effect on the stress intensity factor at the crack tip. The results show that the crack tip slope near the crack tip is a more critical parameter than the notch width. Interestingly, making the crack blunt increases the SIF of the load-carrying ply compared to the exact analytical model, $K^L_{Q(A)}$, and it seems to approach $K^L_{Q(B)}$. Basically, when the crack-tip is made blunt, the σ_{xx} stresses ahead of the crack tip reduce, and this is equivalent to β approaching zero. Thus the fracture toughness calculated using the experimental failure loads approach $K^L_{Q(B)}$.

5.5. Effect of local damage near the crack tip

The effects of local damage ahead of the crack tip in the form of delamination and fiber splitting were studied by using a three-dimensional finite element model. It has been noted that for tension loaded laminates, local damage is produced ahead of the crack tip in the form of the matrix cracks in the off-axis plies, splitting in 0° plies and some delamination [3]. This local damage acts as a stress-relieving mechanism and relieves some portion of the high stress in the non-load-carrying plies and transfer more stresses to the load-carrying ply. In the present finite element model, these two types of damage were modeled. All aspects of the finite element model were kept the same as in the sub-model except for the ply interface. Duplicate nodes are placed on either side of ply interfaces, where delamination is expected. To

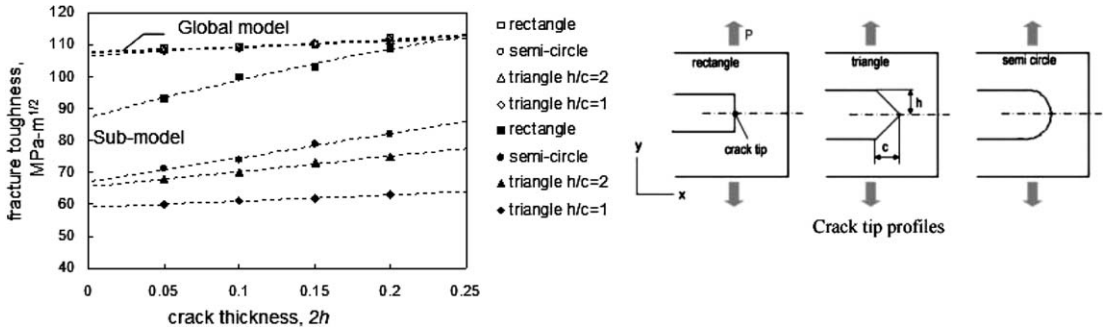

Fig. 7. Effect of crack tip shape on fracture toughness of the load-carrying ply 2D FE global and sub-model results for $[0/\pm45]_s$ laminates.

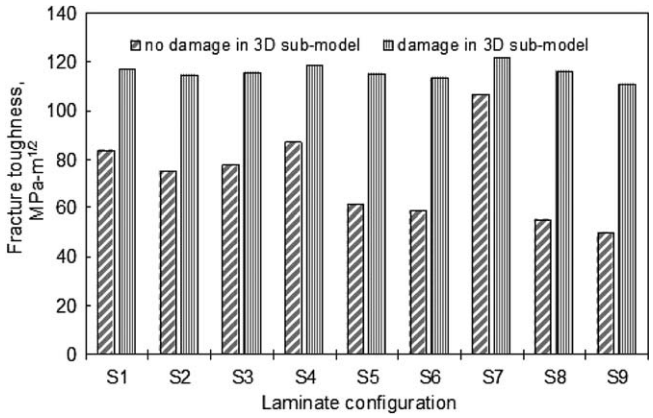

Fig. 8. Effect of local damage on the stress intensity factor in the load-carrying ply.

Table 4
Comparison of the fracture toughness of load-carrying ply obtained from 3D FE model including local damage and an approximate analytical model

Specimen	3D FE analysis (MPa$\sqrt{\text{m}}$)	Analytical model (MPa$\sqrt{\text{m}}$)
S1	116.65	115.66
S2	114.23	108.82
S3	115.71	106.43
S4	118.16	112.62
S5	115.21	109.97
S6	113.53	111.52
S7	121.40	109.04
S8	116.01	123.66
S9	110.51	126.58
Average	115.71	113.81
Standard deviation	3.03	6.95

estimate the delamination area, simple delamination criterion based on maximum interfacial stresses was implemented in ABAQUS by means of a UVAR user subroutine. Similar method was used to estimate axial splitting area, where reduced stiffness property was implemented. A critical stress of 75 MPa was used based on typical epoxy yield stress values. The effect of local damage on the fracture toughness of load carrying ply is depicted in Fig. 8. Again one can note that introducing damage in the crack tip region is similar to that due to crack bluntness described in the preceding section and it increases the stress intensity factor in the load-carrying ply. Further, the fracture toughness evaluated after introduction of damage is more or less uniform in all laminate configurations and it approaches $K^L_{Q(B)}$.

6. A modified analytical model

The SIF of the load-carrying ply, K^L_I, can be computed by using a detailed 3D FE analysis, which can model local damage modes such as fiber splitting and delamination that occurs prior to fracture. Then the SIF of the load-carrying ply can be calculated accurately, and its value corresponding to the laminate failure load represents the layer-independent fracture toughness of the particular material system. The results from this model are presented in Column 2 of Table 4. One can note that the standard deviation in the result is 3.03 MPa$\sqrt{\text{m}}$.

On the other hand, a simpler analytical model could be used. We will call this the modified analytical model. Basically Eq. (1) is used to calculate the laminate fracture toughness from the failure load of the laminate with Eq. (16) for the finite-width correction factor. Then, Eq. (15) is used to calculate the load-carrying ply fracture toughness, which is then the layer-independent fracture toughness of the material system. It should be mentioned that Eq. (15) was obtained from the exact Eq. (14a) by setting $\beta = 0$ which takes into account the effects of local damage at the crack tip. Results from this analytical model are shown in Column 3 of Table 4. The standard deviation for K^L_Q obtained using this analytical model is 6.95 MPa$\sqrt{\text{m}}$ (see Fig. 9).

Using the mean value of 113.81 MPa$\sqrt{\text{m}}$ for K^L_Q, the laminate fracture toughness $\overline{K}_Q$ was calculated using Eq. (15), and they are compared with the experimental results for various laminates in Fig. 10. The results are presented in terms of the parameter η introduced by Sun et al. [3]. The variable η was defined as the ratio of the stress intensity factor of the load-carrying ply to the average laminate stress intensity factor, when β is taken as zero, and can be obtained from Eq. (15) as

$$\eta = t[\overline{Q}^L_{12}A^*_{12} + \overline{Q}^L_{22}A^*_{22}] \tag{17}$$

It should be noted that η, like β, depends only on the laminate properties. Good agreement is observed between the experiments and predictions. This is not surprising because

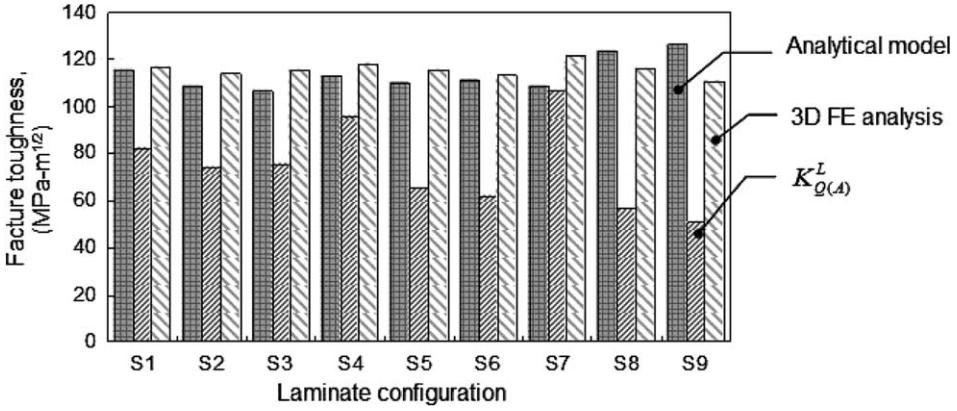

Fig. 9. Comparison of fracture toughness of load-carrying ply computed using the finite element method, the analytical model of Eq. (14a) and the modified analytical model.

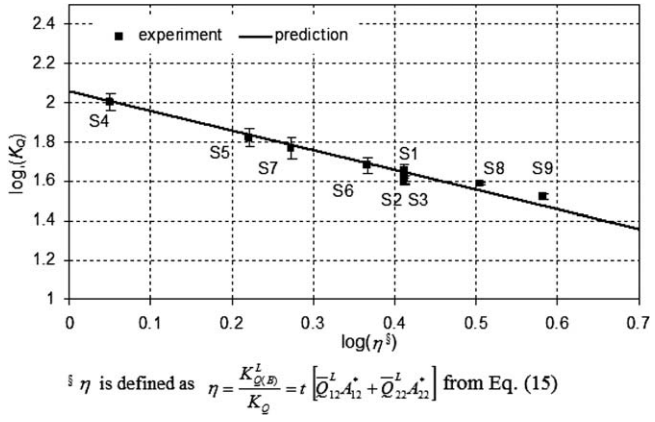

Fig. 10. Comparison of experimental results with model predictions.

K^L_Q itself has been calculated using the experimental results. Rather the agreement shown in Fig. 10 should be considered as a demonstration of usefulness of the layer-independent fracture toughness concept.

7. Conclusions

The results of fracture tests performed on various graphite/epoxy laminates were analyzed in order to identify a layer-independent fracture parameter as suggested by Sun et al. [3]. The stress intensity factor (SIF) of the load-carrying ply at the instance of failure seems to be the critical parameter for predicting the failure of notched composite laminates. However, the SIF of the load-carrying ply seems to be significantly large compared to the values obtained by detailed three-dimensional finite element analysis. This is due to the fact that the crack tip damage and the bluntness of the cracks relive the stresses in other plies and increase the stress in the load-carrying ply. Furthermore, finite width of the specimen plays a role in the SIF. A simple analytical method is proposed that accounts for the aforementioned effects, and the fracture toughness of laminates with different configurations can be predicted from a single fracture toughness value measured experimentally.

Acknowledgements

This material is based upon work supported by the US Army Research Laboratory and the US Army Research Office under Grant DAAD19-02-1-0330. The support and encouragement of Dr. Bruce LaMattina, grant monitor, is gratefully acknowledged.

References

[1] Awerbuch J, Madhukar MS. Notched strength of composite laminates: prediction and experiments – a review. J Reinf Plast Compos 1985;4:3–159.
[2] Whitney JM, Nuismer RJ. Stress fracture criteria for laminated composites containing concentrations. J Compos Mater 1974;8:253–65.
[3] Vaidya RS, Sun CT. Fracture criterion for notched thin composite laminates. AIAA J 1997;35(2):311–4.
[4] Vaidya RS, Klug JC, Sun CT. Effect of ply thickness on fracture of notched composite laminates. AIAA J 1988;36(1):81–8.
[5] Sih GC, Liebowitz H, editors. Mathematical theories of brittle fracture in fracture an advance treastise, vol. II. New York: Academic Press; 1968.
[6] ABAQUS version 6.2. Theory manual. Hibbit, Karlsson and Sorensen Inc., Pawtucket (RI).
[7] Sankar BV, Sonik V. Pointwise energy release rate in delaminated plates. AIAA J 1995;33(7):1312–8.
[8] Tan SC. Finite-width correction factors for anisotropic plate containing a central opening. J Compos Mater 1998;22:1080–98.